analytical chemistry

Article

pubs.acs.org/ac

Gas-Phase FRET Efficiency Measurements To Probe the Conformation of Mass-Selected Proteins

Martin F. Czar,[§] Franziska Zosel,[†] Iwo König,[†] Daniel Nettels,[†] Bengt Wunderlich,[†] Benjamin Schuler,[†] Arash Zarrine-Afsar,*[,†,‡] and Rebecca A. Jockusch*[,§]

[§]Department of Chemistry, University of Toronto, Toronto, Ontario M5S 3H6, Canada

[†]Biochemisches Institut, Universität Zürich, Zürich, CH-8057, Switzerland

Supporting Information

ABSTRACT: Electrospray ionization and mass spectrometry have revolutionized the chemical analysis of biological molecules, including proteins. However, the correspondence between a protein's native structure and its structure in the mass spectrometer (where it is gaseous) remains unclear. Here, we show that fluorescence (Förster) resonance energy transfer (FRET) measurements combined with mass spectrometry provides intramolecular distance constraints in gaseous, ionized proteins. Using an experimental setup which combines trapping mass spectrometry and laser-induced fluorescence spectroscopy, the structure of a fluorescently labeled mutant variant of the protein GB1 was probed as a function of charge state. Steady-state fluorescence emission spectra and time-resolved donor fluorescence measurements of mass-selected GB1 show a marked decrease in the FRET efficiency with increasing number of charges on the gaseous protein, which suggests a Coulombically driven unfolding and expansion of its structure. This lies in stark contrast to the pH stability of GB1 in solution. Comparison with solution-phase single-molecule FRET measurements show lower FRET efficiency for all charge states of the gaseous protein examined, indicating that the ensemble of conformations present in the gas phase is, on average, more expanded than the native form. These results represent the first FRET measurements on a mass-selected protein and illustrate the utility of FRET for obtaining a new kind of structural information for large, desolvated biomolecules.

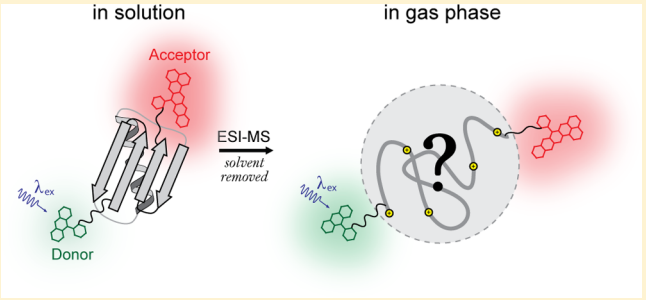

The combination of soft ionization methods such as electrospray ionization (ESI)[1,2] and trapping mass spectrometry (MS) has enabled detailed studies on the reactivity and structure of proteins in the gas phase. However, better understanding the transferability of physical and chemical properties measured *in vacuo* to their native (*in vivo*) or near-native environments remains an intense area of research.[3,4] This research is motivated largely by two factors. First, determining how, and under what conditions, a desolvated protein's structure is different from what is found in nature may reveal the structural importance of those interactions which are removed upon transfer to the gas phase. Further, inferences drawn based upon MS data about solution-phase properties demand a clear understanding of the relationship between the solution- and gas-phase behavior of proteins. The available tools to study gas-phase structure in proteins, including those relying on ion mobility,[5] deuterium exchange,[6] and ion dissociation,[7,8] have been used to glean significant insight: electrosprayed proteins carrying a relatively low number of charges often retain facets of their solution structure, whereas those carrying more charge lose these characteristics. Furthermore, larger proteins and protein assemblies appear to be more likely to retain structure upon electrospray ionization than their smaller counterparts, perhaps due to enhanced kinetic trapping of the larger systems. Despite these advances, the richness in structural detail that is routinely attainable for proteins in solution is lacking for gaseous proteins due to the limitations of available tools for gas-phase structural characterization. Here, we show that spectral (dispersed) and time-resolved fluorescence (or Förster) resonance energy transfer (FRET) measurements can be used to obtain intramolecular distance constraints in gaseous protein ions.

FRET is the nonradiative transfer of electronic energy from an excited donor dye to an acceptor dye in its ground state and occurs through dipole−dipole interactions.[9,10] This process results in a quenching of donor fluorescence, sensitized emission from the acceptor, and a transfer rate which depends strongly (inverse sixth-power) on the distance between the dyes. Thus, the efficiency of energy transfer, which encodes structural information, can be assessed both by steady-state spectral fluorescence measurements and by measurement of time-resolved fluorescence. The latter is generally regarded as more robust for the determination of FRET efficiencies. The effective working distance of FRET is in the range of 2−10 nm,

Received: April 27, 2015
Accepted: June 25, 2015
Published: June 25, 2015

DOI: 10.1021/acs.analchem.5b01591
Anal. Chem. 2015, 87, 7559−7565

which spans well the dimensions of many biological systems; FRET has thus become a popular way to study biological processes in solution, including protein folding[11−13] and protein−protein interaction.[14] The exquisite sensitivity of FRET makes it well-suited for studying protein dynamics in solution on the submicrosecond to millisecond time scales at the single-molecule level;[13] this sensitivity also makes it an attractive choice for gas-phase analysis, where low ion density and low light collection efficiency forestall the use of less sensitive optical methods.

In the gas phase, FRET has so far only been applied to study small, model systems. Seminal work reported in 2003 by the group of J. H. Parks employed FRET to probe the temperature-dependent unzipping of complementary 14-mer oligonucleotides in a quadrupole ion trap mass spectrometer.[15] Subsequent work from the Zenobi lab utilized a FRET scheme to probe short synthetic polymers in a Penning trap.[16] Both of these early works relied on measurement of total donor fluorescence, from which FRET efficiencies (and thus interdye distances) could not be obtained. The main challenge to the measurement of gas-phase FRET efficiencies is the collection of sufficient fluorescence signal that the light may be spectrally dispersed and/or that time-resolved measurements may be performed in a reasonably efficient manner. This challenge generally grows with the size of the system examined because space charge limits the total density of charges which may be trapped,[17] and larger systems (at least those transferred to the gas phase via ESI) generally carry more charges. Recently, an elegant "action-FRET" strategy was proposed by the Dugourd group as a means to circumvent the need for optical detection.[18] While action FRET shows promise and is more easily implemented than traditional FRET, optical detection has the distinct advantage of providing a way to resolve multiple conformational populations which display different FRET efficiencies, i.e., via time-resolved fluorescence measurements. This was shown recently by our group in a study on dye-labeled model peptides containing 8, 14, and 20 prolines,[19] which also reported the first values of gas-phase FRET efficiencies.

Here, we report the first FRET measurements of a gaseous ionized protein, namely, a 59-residue variant of the immunoglobin G-binding domain of protein G (GB1) (sequence shown in the Supporting Information). It has a common (ubiquitin-like) structural motif comprised of a four-stranded β-sheet, which is spanned by a single α-helix, thus forming a densely packed hydrophobic core (Scheme 1).[20] The

Scheme 1. X-ray Crystal Structure of GB1 (from 1PGA)[20] with Modifications for Fluorescent Labeling Indicated

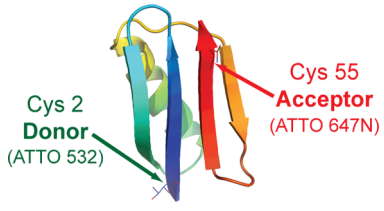

structural and dynamic properties of GB1 have been studied in detail in the condensed phase, notably by X-ray crystallography,[20] nuclear magnetic resonance spectroscopy,[21−24] stopped-flow kinetics experiments,[25−27] differential scanning calorimetry,[28] and computational methods.[29] GB1 has high thermal stability, with a melting temperature of 87.5 °C at pH 5.4,[28] and it retains its native fold over a broad pH range (1.5−11).[25] The solution-phase stability of GB1 has been attributed to its high secondary structure content (∼95%) and the amphiphilic helix which is involved in the formation of its hydrophobic core.[21,24,28] These features led us to ask whether the fold of GB1 remains intact in the gas phase, where removal of solvent may be expected to shift the balance of the enthalpic and entropic contributions which maintain its native fold.

The gas-phase FRET experiments described below use a combination of electrospray ionization, trapping mass spectrometry, and fluorescence spectroscopy to probe the gas-phase structure of a fluorescently labeled mutant variant of the protein GB1. The FRET efficiency of the gaseous protein is investigated as a function of charge state using both dispersed (spectral) fluorescence measurements and time-resolved fluorescence from the donor dye. Gas-phase FRET efficiencies, and derived distance constraints, are compared with results from solution-phase single-molecule FRET experiments.

EXPERIMENTAL SECTION

To enable gas-phase FRET investigations, a GB1 variant was employed which has two residues substituted with cysteine near its termini, at Asn 2 and Thr 55. These residues are located within beta strands and are surface exposed, so these substitutions should be relatively benign.[30] The substitutions enabled site-selective labeling with two thiol-reactive dyes: ATTO 532 (donor, D) and ATTO 647N (acceptor, A) (Scheme 1, protocol in the Supporting Information, Figure S-1). The conjugate GB1-D contains only the donor dye, whereas GB1-DA has both donor and acceptor labels.

Fluorescence emission spectra and lifetime measurements of gaseous GB1 conjugates employed a mass spectrometry setup with modifications to enable spectroscopic investigations of mass-selected gaseous ions.[31−33] Central to the setup is a quadrupole ion trap mass spectrometer (QIT, *Esquire 3000+*, Bruker Daltonics, Bremen, Germany) which has holes drilled in the ring electrode for optical access. The use of a QIT enables confinement of a relatively large number of mass-selected ions (up to ∼100 000) for up to 20 s in a much smaller (∼0.1 mm^3) volume[34] than other types of trapping mass spectrometers, which facilitates the collection of fluorescence. The trade-off for the relatively high fluorescence signal achievable with the high ion densities in our setup is a reduction of mass resolving power of the QIT, which is already substantially lower than that of Orbitraps and Penning traps. Ions trapped in the QIT are irradiated with UV/visible light (tunable from 350−530 nm) generated by frequency-doubling the output of a pulsed (∼130 fs pulse duration, 80 MHz repetition rate) titanium:sapphire laser (*Tsunami*, Spectra-Physics, Newport Co., Mountainview, USA). This choice of laser system was guided by the need for both wavelength tunability and a pulsed source with a high repetition rate. The latter is critical for efficient measurement of fluorescence lifetimes using time-correlated single-photon counting (TCSP) techniques, which we employ due to their compatibility with low levels of light.[33]

Nanoelectrospray ionization (nano-ESI)[2] was used to deliver GB1 conjugates with multiple sodium adducts (of type $[\text{GB1-DA} + m\text{Na} - (m \mp n)\text{H}]^{n\pm}$) to the mass spectrometer (experimental details in the Supporting Information). These were trapped, and mass selection was used to isolate complexes with a known number of charges. These complexes were then irradiated for 0.5−10 s using 485 nm light (∼10 mW, fwhm = 3.5 nm). Fluorescence emission spectra were measured during

DOI: 10.1021/acs.analchem.5b01591
Anal. Chem. 2015, 87, 7559−7565

the irradiation period by focusing the collected fluorescence light onto the entrance slit of a spectrograph interfaced with an electron-multiplying charge-coupled device (*Shamrock 303i* and *Newton* EM-CCD, Andor Technologies, Belfast, Ireland). Donor fluorescence lifetimes were measured using TCSPC techniques by focusing filtered fluorescence light onto a single-photon avalanche diode (*PDM-100*, Micro Photon Devices, Bolzano, Italy) detector, whose output is sent to a TCSPC card (*TimeHarp 200*, Picoquant, Berlin, Germany). After each irradiation period, a mass spectrum was recorded to ensure that significant photodissociation or electron photodetachment did not occur. Gas-phase fluorescence data shown were acquired from interrogating hundreds of populations of trapped ions and subtracting background light levels measured without ions present. To complement gas-phase experiments, solution-phase single-molecule FRET experiments were carried out on GB1-DA using an experimental setup described previously[35] (see the Supporting Information for details).

RESULTS AND DISCUSSION

Figure 1 shows typical nano-ESI mass spectra, measured in positive ion mode, of protein GB1 containing donor and acceptor labels (GB1-DA) before (top) and after (bottom) isolation of a single charge state. The appearance of the nano-ESI mass spectrum, which features a narrow distribution of charge states centered around the 5+ state, suggests the presence of a folded protein in solution (i.e., at the beginning of the ESI process).[36] The noticeable envelope of peaks within each charge state (inset) corresponds to multiple (0−13) sodium adducts; this was verified by high resolution Fourier-transform ion cyclotron resonance mass spectrometry. The extent of sodium adduction reflects the presence of sodium phosphate in the electrosprayed solution. Solutions without sodium phosphate produced a similar charge-state distribution (Figure S-2, Supporting Information); however, the ESI signal from solutions lacking sodium was not stable for long enough to perform gas-phase fluorescence measurements.

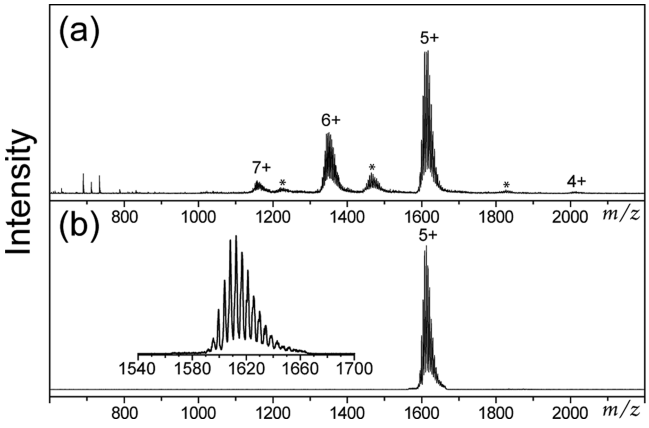

Figure 1. Nanoelectrospray ionization mass spectra of 1 μM GB1-DA in 30 mM ammonium acetate, 0.5 mM sodium phosphate, 80:20 water/methanol. (a) Mass spectrum without ion isolation; the charge states of GB1-DA observed are indicated. Peaks marked with an asterisk (*) correspond to the donor-only conjugate GB1-D present in the sample. (b) Mass spectrum measured after isolation of the 5+ charge state of GB1-DA. Inset is an expansion showing multiple sodium adducts.

Figure 2a−e shows gas-phase fluorescence emission spectra measured for a range of charge states (4+−8+) of GB1-DA generated by positive nano-ESI. There are two bands in all spectra, with maxima at 539 and 640 nm, corresponding to donor and acceptor emission, respectively. Measured spectra of the control donor-only labeled conjugate GB1-D (Figure S-3a, Supporting Information) show a single band at 539 nm, whereas spectra of GB1-A show negligible intensity under the same conditions, indicating that the excitation wavelength used (485 nm) selectively excites the donor. Emission spectra for the 4+ and 5+ states are similar (Figure 2a,b) and indicate a high FRET efficiency, with both showing predominantly sensitized emission from the acceptor, and low intensity from the donor. In contrast, the 6+, 7+, and 8+ states (Figure 2c−e) show a consistent decrease in FRET efficiency with increasing charge, as evidenced by a progressive recovery of donor fluorescence, and a concomitant decrease in acceptor emission intensity. In the 8+ state, very little energy transfer is observed. These results suggest that the higher charge state (6+, 7+, 8+) conformational ensembles represent GB1-DA structures in which the termini of the protein are progressively farther apart with increasing charge, whereas the two lowest charge states examined (4+, 5+) represent structures which are on average more compact. The charge-state dependence of FRET efficiency is similar to that observed previously by our group in small polyproline peptides of intermediate length (14 repeats)[19] and is in accordance with the view of an expansion of the protein's conformation driven by electrostatic repulsion. This effect is magnified in the gas phase due to the absence of charge screening, which is provided by solvent in the condensed phase. Although there are no reports of gas-phase structural studies of GB1 to allow comparison of these data, a clear comparison can be drawn with ion mobility measurements on the protein ubiquitin,[37] which is a protein of similar size and structural topology to GB1. The collision cross section of ubiquitin increases by ∼50% as its charge state increases from 4+ to 8+, shifting from a cross section that is marginally larger than that of the crystal structure to an elongated conformation.

FRET provides an additional nonradiative decay channel for the donor to return to the ground state and manifests as a shortening of the donor fluorescence lifetime. Fluorescence time-decays measured for the donor channel (isolated using a 506−594 nm band-pass filter) for the 5+, 6+, and 7+ charge states of gaseous GB1-DA are shown in Figure 2f−h, with fits shown in green. Donor lifetimes are clearly shorter in the presence of the acceptor than in its absence (i.e., in GB1-D), where the lifetime is ∼7.9 ns (overlaid gray traces). Furthermore, the measured decay depends on charge state for GB1-DA, while it is insensitive to the charge state for GB1-D (Figure S-3b−e, Supporting Information). Lifetimes extracted from fits to the time-resolved data are listed in Table 1. The 5+ state (Figure 2f) exhibits a clear multi-exponential decay, with a fast major decay component (62% from fitted amplitude) with a lifetime of 1.05 ± 0.11 ns, and a slower minor component (30% from fitted amplitude) with a fitted lifetime of 4.3 ± 1.5 ns. The remaining 8% fitted amplitude corresponds to a component included in the fit with a lifetime fixed at 7.9 ns. This was done in order to account for the possibility of a population that is FRET-inactive due, e.g., to residual inactivation of the acceptor by intramolecular electron transfer,[38] which if present and unaccounted for, would result in erroneously long fitted lifetimes. The data suggest that at least two conformational ensembles are resolved in the isolated 5+

DOI: 10.1021/acs.analchem.5b01591
Anal. Chem. 2015, 87, 7559−7565

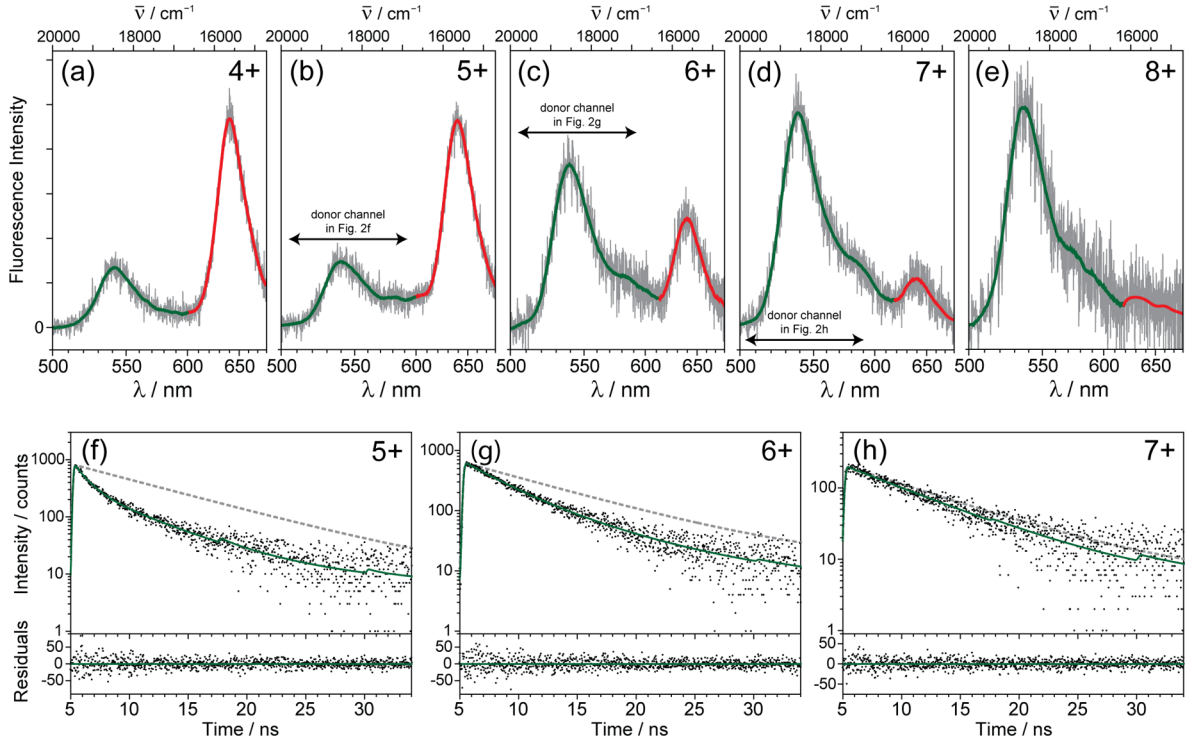

Figure 2. Charge-state resolved emission spectra (a–e) and donor band time-resolved fluorescence (f–h) of fluorescently labeled gaseous GB1-DA conjugates produced by nanoelectrospray ionization and excited with 485 nm light. Smoothed lines in spectra highlight the donor (green) and acceptor (red) emission bands. The wavelength range transmitted by the band-pass filter used in donor lifetime measurements is indicated. Fits to the time-resolved data (f–h, solid curves) are multiexponential functions convolved with a Gaussian instrument response function of adjustable width (~0.2 ns). The extracted fit parameters are shown in Table 1. A small amount of secondary excitation at 12.5 ns intervals, due to incomplete pulse picking, is visible as small bumps in the time-resolved data and has been accounted for in the fit. More slowly decaying traces (dashed gray lines) show the longer lifetime of the donor-only construct, GB1-D (see the Supporting Information).

Table 1. Computed Gas-Phase FRET Efficiencies (E) and Inter-Dye Distance Estimates (r_{DA}) for Different Charge States of GB1-DA

	fluorescence spectra		time-resolved donor fluorescence			
charge state	E^a	$r_{DA}{}^b$ (Å)	relative amplitude	lifetime (ns)	E^a	$r_{DA}{}^b$ (Å)
4+	0.77 ± 0.05	54 ± 4	–	–	–	–
5+	0.76 ± 0.05	55 ± 4	A_1 = 0.62 ± 0.07	τ_1 = 1.05 ± 0.11	E_1 = 0.87 ± 0.02	r_{DA1} = 45 ± 2
			A_2 = 0.30 ± 0.07	τ_2 = 4.3 ± 1.5	E_2 = 0.44 ± 0.21	r_{DA2} = 90 ± 30
			$A_0{}^d$ = 0.08 ± 0.11		$E_{avg}{}^c$ = 0.72 ± 0.20	
6+	0.38 ± 0.06	94 ± 8	A_1 = 0.71 ± 0.06	τ_1 = 3.35 ± 0.21	E_1 = 0.57 ± 0.04	r_{DA1} = 72 ± 4
			$A_0{}^d$ = 0.29 ± 0.05		$E_{avg}{}^c$ = 0.32 ± 0.14	
7+	0.14 ± 0.03	150 ± 15	–	τ_1 = 6.59 ± 0.22	0.16 ± 0.07	150 ± 30
8+	0.06 ± 0.02	>170	–	–	–	–
4–	0.89 ± 0.03	43 ± 3	–	–	–	–
5–	0.83 ± 0.05	49 ± 5	–	–	–	–

[a]Procedures for calculations are outlined in the Supporting Information. [b]Calculated using measured FRET efficiencies (E), a Gaussian chain model,[41] and $R_{0,gas}$ = 72 ± 1 Å (see the Supporting Information). [c]Amplitude-weighted average. [d]Relative amplitude of FRET-inactive component, with lifetime fixed at 7.9 ns. This component was not resolvable for the 7+ state, due to its long fluorescence lifetime and relatively low signal-to-noise.

state of GB1-DA: the majority of ions have fast energy transfer due to their relatively compact structures, but a significant fraction have more expanded conformations. Fits to the 6+ data resolve only a single population displaying FRET, with a lifetime of 3.35 ± 0.21 ns. This falls within the uncertainty of the slower minor component from the 5+ data. The 7+ data are fit well by a single exponential decay with a significantly longer lifetime of 6.6 ns. Overall, fits to the time-resolved data are consistent with the fluorescence emission spectra (Figure 2a–e), again indicating that the FRET efficiency decreases as the number of charges present on the protein increases. However, analysis of time-resolved data can reveal the presence of multiple conformations, as it does here for the 5+ charge state, information not attainable from steady-state spectra alone. We note that the analysis presented here used a discrete number of (up to three) lifetime components. Time-resolved fluorescence from an ensemble of conformations is better modeled using a continuous interdye distance distribution function; however, given the relatively low signal-to-noise for these gas-phase fluorescence measurements, such treatment was not feasible.

DOI: 10.1021/acs.analchem.5b01591
Anal. Chem. 2015, 87, 7559–7565

We have also examined the fluorescence properties of two charge states of GB1-DA generated by negative nano-ESI (Figure 3). Both anionic charge states show sensitized emission

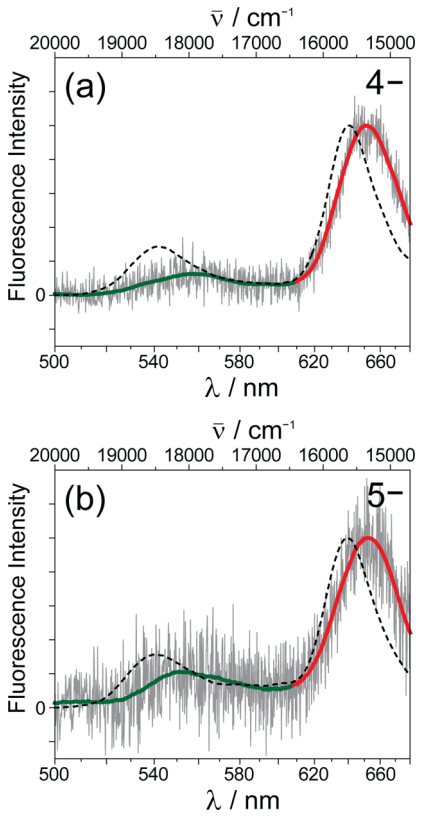

Figure 3. Fluorescence emission spectra (gray traces) for 4− (a) and 5− (b) charge states of GB1-DA, excited using 485 nm light. Smoothed lines highlight donor (green) and acceptor (red) emission bands. Smoothed emission spectra of the 4+ (a) and 5+ (b) states (dashed lines) are overlaid for comparison.

from the acceptor, with a smaller band corresponding to fluorescence from the donor. The emission maxima of the donor and acceptor dyes are shifted to somewhat lower energy, by 500 and 200 cm^{-1}, respectively, than their cationic counterparts. The FRET efficiencies in the 4− and 5− states are slightly higher than those of the 4+ and 5+ states, suggesting anionic GB1-DA conformers which are perhaps marginally more compact than the cations.

The signal-to-noise in the emission spectra measured for the anionic GB1-DA species (Figure 3), and also for the higher charge states of the cations (Figure 2c−e), is noticeably worse than in the spectra measured for lower charge states of cationic GB1-DA (*cf.* Figure 2a,b). In the case of the anions, this is a result of facile electron photodetachment (*e*PD)[39] from negatively charged GB1-DA, which is discernible in the measured mass spectrum. This is not unexpected, as the photon energy (2.55 eV) at the irradiation wavelength used is sufficient to detach electrons from other multiply charged anionic proteins with similar charge density, in both highly folded and elongated conformations.[40] Unfortunately, the facile *e*PD reduces the maximum allowable irradiation time significantly in these experiments (~0.5 s, *cf.* 10 s irradiation for the 4+ and 5+ charge states), which hinders the duty cycle of fluorescence measurements. FRET measurements of the more highly charged cations (6+, 7+, 8+) similarly suffer from duty cycle limitations, although in this case too much irradiation results in undesired photofragmentation rather than electron detachment. The significantly lower relative abundances for the higher charge states (as expected for an electrosprayed protein under "native" solution conditions; see Figure 1) also decreased the signal-to-noise of the 7+, and 8+ charge states.

The structural information we seek (i.e., interdye distances) depends on the FRET efficiency (E), which can be calculated from emission spectra or more reliably from the donor fluorescence lifetimes (Table 1; see the Supporting Information for calculations). In cationic GB1-DA, the FRET efficiency computed from spectra is highest for the 4+ and 5+ states (~0.8), lies at an intermediate value for the 6+ state (~0.4), and then declines to below 0.2 for the 7+ and 8+ states. In the 4− and 5− states, the efficiencies lie near 0.9 and 0.8, respectively. Interdye distances (r_{DA}) for gaseous GB1 were calculated according to Förster theory[9,10] and using a Gaussian chain model.[41] Central to calculating r_{DA} is the Förster radius (R_0), which is the distance at which $E = 0.5$. R_0 for a given dye pair depends upon the spectroscopic properties of the dyes and on their chemical environment. In aqueous solution, R_0 for this dye pair is 59 Å (Atto Tec GmbH); however, its gas-phase value is unknown. Making reasonable assumptions, we estimate $R_{0,gas}$ for this dye pair to be 72 Å (see the Supporting Information for details). This is significantly larger than the solution-phase value due mainly to the lower index of refraction in vacuum ($n_{vacuum} = 1$, while $n_{aq} \approx 1.33$ at 530 nm). We note that the largest uncertainty in our estimate of $R_{0,gas}$ is the orientation factor κ^2, which describes the relative orientation of the donor and acceptor transition dipoles. In solution, polarization anisotropy decay measurements can be used to assess the rotational mobility of a FRET pair,[10] but this is not accessible in our gas-phase experiments. Instead, we have assumed here the dynamically averaged value of $\kappa^2 = 2/3$, as is often done in solution-phase studies. However, the dyes may not be freely rotating in this gas-phase system, especially given that they are charged (see the Supporting Information for further discussion).

Table 1 shows estimates of interdye distances (r_{DA}) for the various charge states of gaseous GB1-DA, computed using measured FRET efficiencies and the estimated $R_{0,gas}$ value of 72 Å. Estimates range from 40−60 Å for the lowest charge states examined (4+, 5+, 4−, 5−) and are >70 Å for the 6+, 7+, and 8+ states. All of these distances are longer than the interdye distance for the folded protein in the condensed phase as determined by aqueous-phase single-molecule FRET experiments. In aqueous solution at pH 7 and 2.5, energy transfer is virtually complete (Figure S-4, Supporting Information). FRET efficiency histograms suggest values of $r_{DA} < 30$ Å for the folded protein in solution, which agrees well with the inter-residue distance of the dye labeling sites based on the X-ray crystal structure of GB1 (21 Å),[20] plus a correction for the lengths of the dye−protein linkers used. The >70 Å interdye distances in the higher charge states examined (6+, 7+, 8+) and in the expanded population of the 5+ state suggest gaseous GB1 conformations which are significantly expanded relative to its native fold. The sites of dye attachment are 53 residues apart; for comparison, an α-helix of this length would be 79.5 Å.

Just how compact are the populations identified here as relatively compact? Overall, the estimates of r_{DA} may indicate that, even in the most compact gaseous GB1 conformers probed, the sites of dye attachment (which lie on β-strands 1

DOI: 10.1021/acs.analchem.5b01591
Anal. Chem. 2015, 87, 7559−7565

and 4) are not in as close proximity as they are in the folded structure (Scheme 1). The higher efficiency of energy transfer observed for the anionic charge states compared to the most compact cationic charge states supports the idea that the 4+ and more compact 5+ population are more expanded than the native structure in solution. However, given the remaining uncertainties in the orientational freedom of the dyes, the signal-to-noise of the time-resolved data, and inherent challenges of multiexponential fitting, as well as the possibility of residual inactivation of the acceptor by electron transfer,[38] it may be that the most compact gaseous GB1 conformers are indeed close in compactness to the native solution structure. Furthermore, we cannot rule out the possibility that the analysis used for the lifetime data might miss a minor very high FRET component due to its very fast decay. Experiments designed to address this possibility are currently underway in our laboratory. Nonetheless, with increasing number of charges per molecule, a clear transition to unfolded and increasingly expanded conformations is evident, to an extent that prevents energy transfer almost completely.

The gas-phase behavior of GB1-DA lies in contrast to the stability of its fold in solution. The pH stability of wild type GB1[25] translates to stability over charge states in solution ranging approximately from 13− to 7+, assuming standard amino acid pK_a values. Single-molecule FRET data indicate that the fluorescently labeled mutant variant used here is, like the wild type, folded at neutral pH and under acidic conditions (Figure S-4b, Supporting Information). The narrow charge-state distribution and low overall degree of charging observed in the ESI mass spectrum (Figure 1) are consistent with the presence of a folded protein at the start of the ESI process, in agreement with single-molecule data measured in ESI buffer (Figure S-4c, Supporting Information). The gas-phase FRET data shown here suggest that the desolvation and charging processes lead to a disruption of the tertiary structure of GB1-DA on the time scale of these experiments. In some ways, this is not surprising as GB1 lacks several features which favor retention of native-like structure in the gas phase, including disulfide bonds that stabilize tertiary structure and the kinetic stability (arising from the internal energy bath) associated with larger proteins and complexes. Moreover, the energy barrier for unfolding is likely to be lower in the gas phase than in solution due to the enhanced Coulomb repulsion upon desolvation of this small protein.[42] This, combined with the seconds-long irradiation period used in these gas-phase FRET experiments, which are quite long by mass spectrometry standards, could give many small proteins sufficient time to rearrange.

CONCLUSIONS

This work adds a technique complementary to the methods currently available to probe the conformation of mass-selected biomolecules. FRET efficiency measurements provide a probe of interdye distances, which here show the expansion with increasing charge state of the conformation of the small gaseous protein GB1-DA, pointing to a Coulombically-driven structural change in the absence of solvent. Moreover, time-resolved measurements indicate the presence of both expanded and relatively compact conformers for the 5+ charge state.

While the necessity of appropriate labels for FRET experiments is a drawback of this technique, FRET-based strategies are remarkably powerful. Their use in the gas phase will make it possible to access new information about biomolecules. FRET is intrinsically very sensitive to changes in interdye distance near the Förster radius (R_0) for the FRET pair used. Using careful selection of labeling sites, FRET methods can be adapted to target substructural changes via the incorporation of paired labels at different sites, in order to give insight into the cooperativity of structural transitions.[43,44] Furthermore, use of a three-color FRET strategy makes possible the measurement of two distances in concert.[45] We anticipate that distance constraint information obtained using gas-phase FRET will assist computational efforts aimed at larger systems. Ultimately, since relatively little is known about protein folding in the complete (or partial) absence of solvent, we envision using gas-phase FRET of mass-selected proteins and clusters to study several aspects of protein folding, including how destabilizing point mutations translate to the gas phase and how the addition of a well-defined number of water molecules affects protein folding and stability.

ASSOCIATED CONTENT

Supporting Information

GB1 synthesis; mass spectra; donor-only control experiments; calculations; single-molecule FRET experiments. The Supporting Information is available free of charge on the ACS Publications website at DOI: 10.1021/acs.analchem.5b01591.

AUTHOR INFORMATION

Corresponding Authors

*Tel: +1-416-581-8473. E-mail: arash.zarrine.afsar@utoronto.ca.

*Tel: +1-416-946-7198. E-mail: rjockusc@chem.utoronto.ca.

Present Address

‡(A.F.-A.) Techna Institute for the Advancement of Technology for Health, University of Toronto, Toronto, Ontario M5G 1P5, Canada

Notes

The authors declare no competing financial interest.

ACKNOWLEDGMENTS

M.F.C. and R.A.J. are grateful for funding from the Natural Sciences and Engineering Research Council of Canada, the Canada Research Chairs Program, the Canada Foundation for Innovation, and the Province of Ontario. This work was also supported by the Human Frontier Science Program (to A.Z.-A.) and the Swiss National Science Foundation (to B.S.).

REFERENCES

(1) Fenn, J. B.; Mann, M.; Meng, C. K.; Wong, S. F.; Whitehouse, C. M. *Mass Spectrom. Rev.* **1990**, *9* (1), 37−70.
(2) Wilm, M.; Mann, M. *Anal. Chem.* **1996**, *68* (1), 1−8.
(3) Ruotolo, B.; Robinson, C. *Curr. Opin. Chem. Biol.* **2006**, *10*, 402−408.
(4) Breuker, K.; McLafferty, F. W. *Proc. Natl. Acad. Sci. U. S. A.* **2008**, *105* (47), 18145−18152.
(5) Bohrer, B. C.; Merenbloom, S. I.; Koeniger, S. L.; Hilderbrand, A. E.; Clemmer, D. E. *Annu. Rev. Anal. Chem.* **2008**, *1* (1), 293−327.
(6) Wood, T.; Chorush, R.; Wampler, F.; Little, D.; O'Connor, P.; McLafferty, F. *Proc. Natl. Acad. Sci. U. S. A.* **1995**, *92* (7), 2451−2454.
(7) Oomens, J.; Polfer, N.; Moore, D. T.; van der Meer, L.; Marshall, A. G.; Eyler, J. R.; Meijer, G.; von Helden, G. *Phys. Chem. Chem. Phys.* **2005**, *7* (7), 1345.
(8) Oh, H.; Breuker, K.; Sze, S.; Ge, Y.; Carpenter, B.; McLafferty, F. *Proc. Natl. Acad. Sci. U. S. A.* **2002**, *99* (25), 15863−15868.
(9) Förster, T. *Ann. Phys.* **1948**, *437* (1−2), 55−75.
(10) Lakowicz, J. R. *Principles of fluorescence spectroscopy*; Springer: New York, 2006.

DOI: 10.1021/acs.analchem.5b01591
Anal. Chem. 2015, 87, 7559−7565

(11) Royer, C. A. *Chem. Rev.* **2006**, *106* (5), 1769−1784.
(12) Schuler, B.; Lipman, E. A.; Eaton, W. A. *Nature* **2002**, *419* (6908), 743−747.
(13) Schuler, B.; Hofmann, H. *Curr. Opin. Struct. Biol.* **2013**, *23* (1), 36−47.
(14) Dehmelt, L.; Bastiaens, P. I. H. *Nat. Rev. Mol. Cell Biol.* **2010**, *11* (6), 440−452.
(15) Danell, A.; Parks, J. H. *Int. J. Mass Spectrom.* **2003**, *229* (1−2), 35−45.
(16) Dashtiev, M.; Azov, V.; Frankevich, V.; Scharfenberg, L.; Zenobi, R. *J. Am. Soc. Mass Spectrom.* **2005**, *16* (9), 1481−1487.
(17) March, R. E.; Todd, J. F. J. *Quadrupole Ion Trap Mass Spectrometry*; J. Wiley: Hoboken, N.J., 2005.
(18) Daly, S.; Poussigue, F.; Simon, A.-L.; MacAleese, L.; Bertorelle, F.; Chirot, F.; Antoine, R.; Dugourd, P. *Anal. Chem.* **2014**, *86* (17), 8798−8804.
(19) Talbot, F. O.; Rullo, A.; Yao, H.; Jockusch, R. A. *J. Am. Chem. Soc.* **2010**, *132* (45), 16156−16164.
(20) Gallagher, T.; Alexander, P.; Bryan, P.; Gilliland, G. *Biochemistry* **1994**, *33* (15), 4721−4729.
(21) Gronenborn, A.; Filpula, D.; Essig, N.; Achari, A.; Whitlow, M.; Wingfield, P.; Clore, G. *Science* **1991**, *253* (5020), 657−661.
(22) Minor, D.; Kim, P. *Nature* **1994**, *371* (6494), 264−267.
(23) Minor, D. L.; Kim, P. S. *Nature* **1996**, *380* (6576), 730−734.
(24) Kobayashi, N.; Honda, S.; Yoshii, H.; Munekata, E. *Biochemistry* **2000**, *39* (21), 6564−6571.
(25) Alexander, P.; Orban, J.; Bryan, P. *Biochemistry* **1992**, *31* (32), 7243−7248.
(26) Park, S. H.; O'Neil, K. T.; Roder, H. *Biochemistry* **1997**, *36* (47), 14277−14283.
(27) McCallister, E. L.; Alm, E.; Baker, D. *Nat. Struct. Biol.* **2000**, *7* (8), 669−673.
(28) Alexander, P.; Fahnestock, S.; Lee, T.; Orban, J.; Bryan, P. *Biochemistry* **1992**, *31* (14), 3597−3603.
(29) Nauli, S.; Kuhlman, B.; Baker, D. *Nat. Struct. Biol.* **2001**, *8* (7), 602−605.
(30) Tokuriki, N.; Stricher, F.; Schymkowitz, J.; Serrano, L.; Tawfik, D. S. *J. Mol. Biol.* **2007**, *369* (5), 1318−1332.
(31) Bian, Q.; Forbes, M. W.; Talbot, F. O.; Jockusch, R. A. *Phys. Chem. Chem. Phys.* **2010**, *12* (11), 2590−2598.
(32) Forbes, M. W.; Talbot, F. O.; Jockusch, R. A. In *Practical Aspects of Trapped Ion Mass Spectrometry: Applications of Ion Trapping Devices*; March, R. E., Todd, J. F. J., Eds.; CRC Press: Boca Raton, Florida, 2009; Vol. *5*, Chapter 9, pp 239−290.
(33) Nagy, A. M.; Talbot, F. O.; Czar, M. F.; Jockusch, R. A. *J. Photochem. Photobiol., A* **2012**, *244*, 47−53.
(34) Talbot, F. O.; Sciuto, S. V.; Jockusch, R. A. *J. Am. Soc. Mass Spectrom.* **2013**, *24* (12), 1823−1832.
(35) Hofmann, H.; Hillger, F.; Pfeil, S. H.; Hoffmann, A.; Streich, D.; Haenni, D.; Nettels, D.; Lipman, E. A.; Schuler, B. *Proc. Natl. Acad. Sci. U. S. A.* **2010**, *107* (26), 11793−11798.
(36) Chowdhury, S.; Katta, V.; Chait, B. *J. Am. Chem. Soc.* **1990**, *112* (24), 9012−9013.
(37) Valentine, S. J.; Counterman, A. E.; Clemmer, D. E. *J. Am. Soc. Mass Spectrom.* **1997**, *8* (9), 954−961.
(38) Dietrich, A.; Buschmann, V.; Muller, C.; Sauer, M. *Rev. Mol. Biotechnol.* **2002**, *82* (3), 211−231.
(39) Antoine, R.; Dugourd, P. *Phys. Chem. Chem. Phys.* **2011**, *13* (37), 16494−16509.
(40) Vonderach, M.; Winghart, M.-O.; MacAleese, L.; Chirot, F.; Antoine, R.; Dugourd, P.; Weis, P.; Hampe, O.; Kappes, M. M. *Phys. Chem. Chem. Phys.* **2014**, *16* (7), 3007−3013.
(41) Hoffmann, A.; Kane, A.; Nettels, D.; Hertzog, D. E.; Baumgaertel, P.; Lengefeld, J.; Reichardt, G.; Horsley, D. A.; Seckler, R.; Bakajin, O.; Schuler, B. *Proc. Natl. Acad. Sci. U. S. A.* **2007**, *104* (1), 105−110.
(42) Breuker, K.; Oh, H. B.; Horn, D. M.; Cerda, B. A.; McLafferty, F. W. *J. Am. Chem. Soc.* **2002**, *124* (22), 6407−6420.
(43) Lillo, M. P.; Szpikowska, B. K.; Mas, M. T.; Sutin, J. D.; Beechem, J. M. *Biochemistry* **1997**, *36* (37), 11273−11281.
(44) Sinha, K. K.; Udgaonkar, J. B. *J. Mol. Biol.* **2007**, *370* (2), 385−405.
(45) Hohng, S.; Joo, C.; Ha, T. *Biophys. J.* **2004**, *87* (2), 1328−1337.

DOI: 10.1021/acs.analchem.5b01591
Anal. Chem. 2015, 87, 7559−7565

Supporting Information for:

Gas-phase FRET Efficiency Measurements to Probe the Conformation of Mass-Selected Proteins

submitted to *Analytical Chemistry*

Martin F. Czar,[§] Franziska Zosel,[†] Iwo König,[†] Daniel Nettels,[†] Bengt Wunderlich,[†] Benjamin Schuler,[†] Arash Zarrine-Afsar,[†‡*] and Rebecca A. Jockusch[§*]

[§] Department of Chemistry, University of Toronto, Toronto, ON M5S 3H6, Canada
[†] Biochemisches Institut, Universität Zürich, Zürich, CH-8057, Switzerland
[‡] Techna Institute for the Advancement of Technology for Health, University of Toronto, Toronto, ON M5G 1P5, Canada

[*] Rebecca A. Jockusch
University of Toronto
Department of Chemistry
Toronto, ON M5S 3H6, Canada
Tel: +1-416-946-7198
Email: rjockusc@chem.utoronto.ca

[*] Arash Zarrine-Afsar
University of Toronto
Techna Institute for the Advancement of Technology for Health
Tel: +1-416-581-8473
Email: arash.zarrine.afsar@utoronto.ca

Contents:

Preparation of fluorescently-labeled protein GB1

Protein sequence for GB1

G A M ^{1}G $C_{(Q)}$ Y K L I L N G ^{10}K T L K G E T T T E ^{20}A V D A A T A E K V
^{30}F K Q Y A N D N G V ^{40}D G E W T Y D D A T ^{50}K T F T V $C_{(T)}$ E

Residues Q2 and T55 were replaced by cysteine as indicated. The N-terminal sequence GAM, which is not found in GB1, originates from the engineered Tobacco Etch Virus (TEV) protease cleavage site.

Mutagenesis and preparation of variants

A GB1 plasmid construct in a modified pET-9d vector[1] was subjected to mutagenesis using a variant of the QuickChange PCR protocol (Stratagene) with forward/reverse primers overlapping at the existing NcoI (for the Q2C variant) and KpnI (for the T55C variant) restriction sites. Prior to transformation, the methylated wild type plasmids were eliminated by DpnI digestion through incubating the PCR reaction with 1µl DpnI (New England BioLabs (NEB)) at 37°C for 3 h. PCR products were then purified using the QIAquick PCR purification kit (Qiagen), and subsequently digested using NcoI or KpnI restriction enzymes in recommended reaction conditions (NEB). Digested plasmids were resolved on a 1% agarose gel, and then gel-purified using the QIAquick Gel Extraction Kit (Qiagen). To increase the transformation efficiency, the gel purified plasmids were self-ligated using T4 DNA ligase (Fermentas) at room temperature for 3 h. Plasmid preparations from clones selected under Kanamycin resistance (50 µg/ml) were made using the GeneJET™ Kit (Fermentas) and subjected to DNA sequencing (Microsynth AG, Switzerland) to verify the presence of mutations. For this, XL1-Blue cells (Agilent) were made heat-shock competent with $CaCl_2$ treatment.

Protein purification

The vector contained a sequence coding for an N-terminal hexahistidine tag followed by a cleavage site for Tobacco Etch Virus (TEV) protease, which allowed Nickel affinity chromatography to be used for the purification of the recombinant protein, and subsequent cleavage by TEV protease to eliminate the hexahistidine tag from the purified protein. Single Q2C and T55C variants, as well as a variant containing Cys (C) at both sites (Q2C-T55C), were prepared as described above and verified by DNA sequencing. The Cys codon was optimized for

expression in *E. coli*. We used Rosetta DE3 cells (Millipore) containing the pRARE plasmid (Millipore) to further boost the expression of GB1.

10 ml of a freshly transformed GB1 overnight culture in Rosetta cells (heat-shock competent) was inoculated in 1 l of 2YT medium (under 50 μg/ml Kanamycin (for GB1 plasmid) and 35 μg/ml Chloramphenicol (for pRARE plasmid), grown at 37°C for ~3 h ($O.D._{600}$ ~ 0.7) and induced at 32°C with 1 mM isopropyl β-D-1-thiogalactopyranoside (IPTG) for 8 h. Cells were harvested at 4,000 rpm for 25 min and frozen at −80°C.

The cell pellet was thawed at 37°C, subsequently dissolved in 80 ml 6 M GuHCl, 100 mM sodium phosphate, 10 mM TrisHCl, 10 mM imidazole, pH 8.0 (binding buffer), and then rocked at room temperature for 1 h to lyse the cells and denature all cellular proteins. Cellular debris and insoluble proteins were then pelleted using centrifugation at 10,000 rpm for 30 min. Supernatant containing the soluble proteins was added to 5 ml of HisPur Ni-NTA agarose slurry (Thermo Scientific), which was pre-equilibrated in the binding buffer above. GB1 was bound to Ni-NTA agarose beads for 1 h at room temperature. Ni-NTA was pelleted using gentle centrifugation at 1,500 rpm for 5 min, and washed with 30 ml of binding buffer (repeated 4 times). GB1 was eluted by incubating the Ni-NTA pellet in 20 ml of 6 M GuHCl, 0.2 M acetic acid, pH 4.5 (elution buffer) for 20 min (rocking at room temperature). Supernatant (after centrifugation at 1,500 rpm for 10 min) containing GB1 was filtered through a 0.45 μm filter (TPP, Switzerland), and refolded through equilibrium dialysis against 4 l of 50 mM sodium phosphate, 300 mM NaCl, pH 7.0 at 4 °C overnight (changing the 4 l dialysis solution every 5 h, for a total of 3 times). A 3 kDa cut off membrane (Spectrum Laboratories) was used for dialysis.

TEV protease (recombinantly produced in house as hexahistidine fusion) was added to GB1 variants in a molar ratio of 50:1 (GB1:TEV) along with dithiothreitol (DTT) to a final concentration of 5 mM. The cleavage of the GB1 hexahistidine tag by TEV protease at 4 °C was monitored through SDS-PAGE analysis (Coomassie and silver staining), and was complete after 6 h.

Digested GB1 variants were dialyzed against 50 mM sodium phosphate, 300 mM NaCl, pH 8.0, as above, and subjected to a second round of Ni-NTA pull down (equilibrated in the same buffer) to remove the cleaved hexahistidine tag as well as the TEV protease. Samples were equilibrated with Ni-NTA at 4°C for 1 h, and were then spun down at 1,500 rpm; the collected supernatant contained GB1 without the hexahistidine tag. Removal of the TEV protease and the

cleaved hexahistidine tag was confirmed by SDS-PAGE analysis (Coomassie and silver staining) on a 12% polyacrylamide gel.

A further round of purification with size exclusion chromatography on a Superdex 75 column (GE HealthCare) was performed in 50 mM potassium phosphate, 100 mM NaCl, 0.5 mM EDTA, at pH 7.5. By monitoring the absorbance at 280 nm, fractions containing GB1 were identified and collected. These were subjected to reversed-phase HPLC on a Reprosil Gold C18 column (Dr. Maisch GmbH, Germany) to remove additional degradation products. Protein samples were reduced with tris(2-carboxyethyl) phosphine (TCEP), diluted in 0.1% trifluoroacetic acid (TFA) and eluted with an acetonitrile gradient (elution range 25–50%). Samples were flash frozen in liquid N_2 and subsequently lyophilized.

Labeling with fluorescent dyes

Lyophilized GB1 Q2C-T55C was taken up in 100 mM potassium phosphate, pH 7.2 under a dry N_2 atmosphere and mixed at a protein:dye molar ratio of 1.0:0.7 with a maleimide derivative of the donor dye ATTO 532 (AttoTec GmbH). Protein concentration was determined using absorbance at 280 nm according to the predicted extinction coefficient of the unfolded GB1 sequence at this wavelength. ATTO 532 was freshly dissolved in dry DMSO through sonication. Labeling at room temperature continued for 3 h in the absence of light under N_2 atmosphere. The reaction was then stopped by addition of β-mercaptoethanol.

The reaction products were purified by reversed-phase HPLC using a (H_2O + 0.1% TFA) / acetonitrile gradient on an Xterra RP 18 column (Waters). Free protein, singly-labeled protein and doubly labeled protein containing the donor dye at both Q2C and T55C sites were identified by comparing the ratio of absorbances at 532 nm to 220 nm across peaks in the chromatograms. Fluorescence of ATTO 532 was also used to confirm labeling. It was possible to resolve the site-specifically labeled donor protein conjugates with our reverse phase HPLC protocol (Figure S-1). The protein fraction S-2 was collected, lyophilized and subjected to tryptic fragment analysis with mass spectrometry (Functional Genomics Centre, University of Zurich), which verified Q2C as the ATTO 532 labeling site. This variant was subsequently labeled with a maleimide derivative of the acceptor dye ATTO 647N, as described above, with a protein:dye molar ratio of 1:3. The donor–acceptor variant (Q2C|ATTO 532 donor–T55C|ATTO 647N acceptor) thus produced was subsequently purified by reversed-phase HPLC, as above; absorbance was

monitored during elution, along with fluorescence from the two dyes as well as the FRET signal between the pair (excitation at 532 nm; emission at 670 nm).

Donor-only (Q2C|ATTO 532) and acceptor-only (T55C|ATTO 647N) variants were prepared from single Cys variants, and subsequently labeled as above with a protein:dye molar ratio of 1:1 for 3 h at room temperature. Reversed-phase HPLC purification using the Xterra RP 18 column (Waters) separated the labeled proteins from the small amount (~2-5%) of unlabeled population.

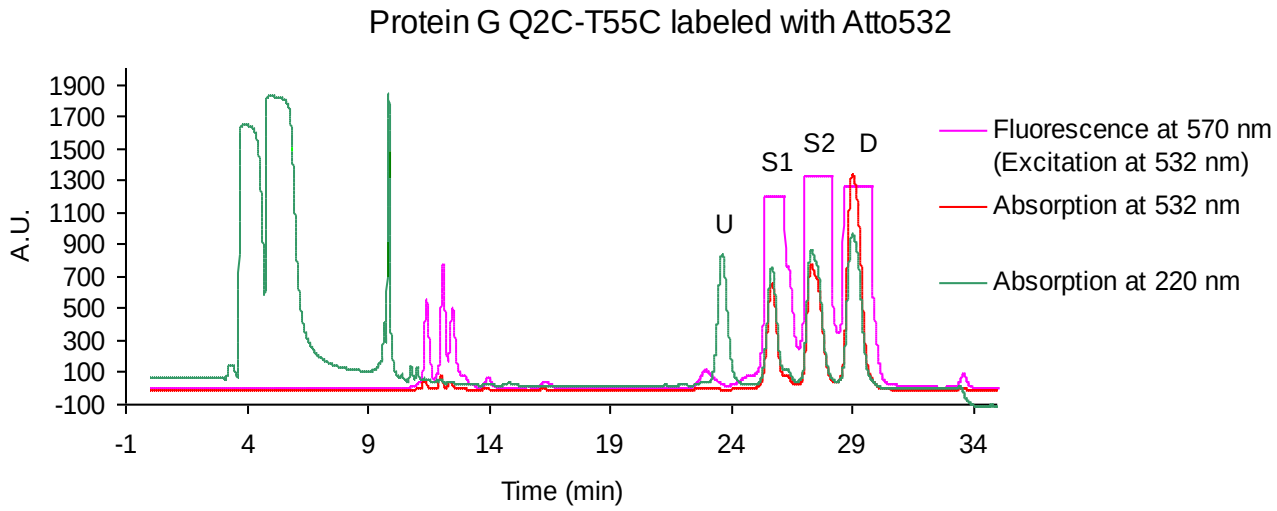

Figure S-1. *Reversed-phase HPLC chromatogram of GB1 Q2C-T55C labeled with ATTO 532*. The labeled peaks correspond to fractions containing unlabeled (U) GB1, singly-labeled (S1 and S2) donor-only GB1 conjugates, and doubly-labeled (D) donor-donor GB1 conjugates. Fraction S2 was confirmed to have ATTO 532 bound at site Q2C by tryptic MALDI analysis, and was used in the second labeling step.

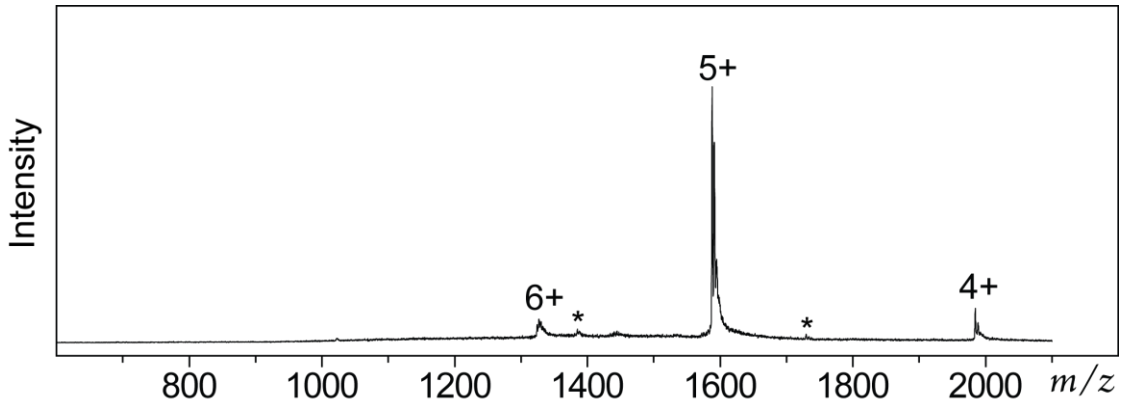

Figure S-2. ESI mass spectrum of 1 μM GB1-DA in 30 mM ammonium acetate, 80:20 water:methanol mixture. Numbers indicate the charge states; peaks labeled with an asterisk (*) correspond to the small amount of donor-only conjugate present in the sample.

Mass Spectrometry

The experimental set-up used to measure laser-induced fluorescence of trapped, mass-selected ions has been detailed elsewhere.[2–4] Below, experimental parameters specific to this study on GB1 are given.

Nano-electrospray ionization was used to deliver GB1–dye conjugates to the quadrupole ion trap (QIT) mass spectrometer. Samples were sprayed at rate of ~10 nL min^{-1} from borosilicate glass capillaries (outer diameter = 1.00 mm, inner diameter = 0.78 mm) that were pulled to an opening size of ~5 μm using a micropipette puller (P-97, Sutter Instrument Co., Novato, CA, USA). Sprayed solutions consisted of 1 μM GB1 conjugate in 80:20 water:methanol mixtures containing 30 mM ammonium acetate and 0.5 mM sodium phosphate. The presence of salt in the electrosprayed samples improved signal stability, and furthermore prevented nano-ESI tips from being clogged by aggregation in the capillary. Figure S-2 shows an ESI mass spectrum of 1 μM GB1 conjugate in 80:20 water:methanol mixtures containing 30 mM ammonium acetate. The charge state distribution is narrow and centered around the 5+ state, which is similar to that measured in the sample containing 0.5 mM sodium phosphate (Figure 1).

Measurement Sequence

The measurement sequence for the detection of fluorescence from trapped ions was as follows. Gaseous, ionized GB1 conjugates generated by nano-ESI were delivered to the trapping region of the QIT by transmission through a heated glass capillary, a skimmer, two octopoles, and two

ion lenses. Ion accumulation times were set to maximally fill the ion trap, and were typically 0.5–3 seconds. The QIT was operated at a helium bath gas pressure of 1.0×10^{-3} mbar (above 8.0×10^{-6} mbar background pressure). Delivered ions were allowed to collisionally cool in the trapping region of the QIT for an additional 50 ms after the end of the ion accumulation period. A sub-population of ions, corresponding to proteins of the desired charge state in complex with 1–16 sodium ions, were isolated using an isolation window of up to 100 *m/z* (Figure S-2c,d). The isolated ions were stored for up to 10 seconds at a parent ion q_z value of 0.59. During the ion storage period, a mechanical shutter was opened, allowing a laser beam to pass through the trapping region of the QIT, thus irradiating the trapped ions. An excitation wavelength of 485 nm was used, with a power ~10 mW. This excitation light was provided by the frequency-doubled output of a pulsed (~130 fs pulse-width), Nd:VO_4-pumped titanium-sapphire laser (Millenia Pro 10sJ pumped Tsunami, Spectra-Physics, Newport Co., Mountainview, USA). For fluorescence lifetime measurements of the donor in GB1-DA and GB1-D, a pulse-picker (Conoptics Model 305, Danbury, CT) was used to reduce the repetition rate of the laser from 80 MHz to 27 MHz, thus giving an observation time window of 37.5 ns for TCPSC measurements; this is more than four times larger than the longest measured lifetime. After irradiation, ions were ejected in order of increasing *m/z* and detected using a conversion dynode in order to measure a mass spectrum. In all cases, the parent ion showed minimal (< 5%) photodissociation, which was assessed by examination of the recorded mass spectrum.

Control Measurements of Singly-Labeled GB1 (GB1-D)

Figure S-3 shows fluorescence emission spectra (a) and fluorescence lifetime measurements (b–e) of fluorescent conjugates of GB1 labeled only with the donor dye. The control donor-only molecule corresponds to fraction S-2 in the chromatogram shown in Figure S-1 (with the donor bound at residue Q2C, as in GB1-DA). The smoothed (fourth-order, 250 point Savitzky-Golay) fluorescence emission spectra for the 4+, 5+, 6+, and 7+ states show very similar spectral shapes, and emission maxima at 539 ± 2 nm. The fluorescence time-decays of the donor for the 4+ (b), 5+ (c), 6+ (d), and 4− (e) charge states were all well-fit by single exponential functions. The extracted fit parameter τ_D, which corresponds to the fluorescence lifetime of the dye, were similar for each charge state. Together, these results suggest no significant changes to the spectroscopic properties of the donor dye with the extent of charging on the protein.

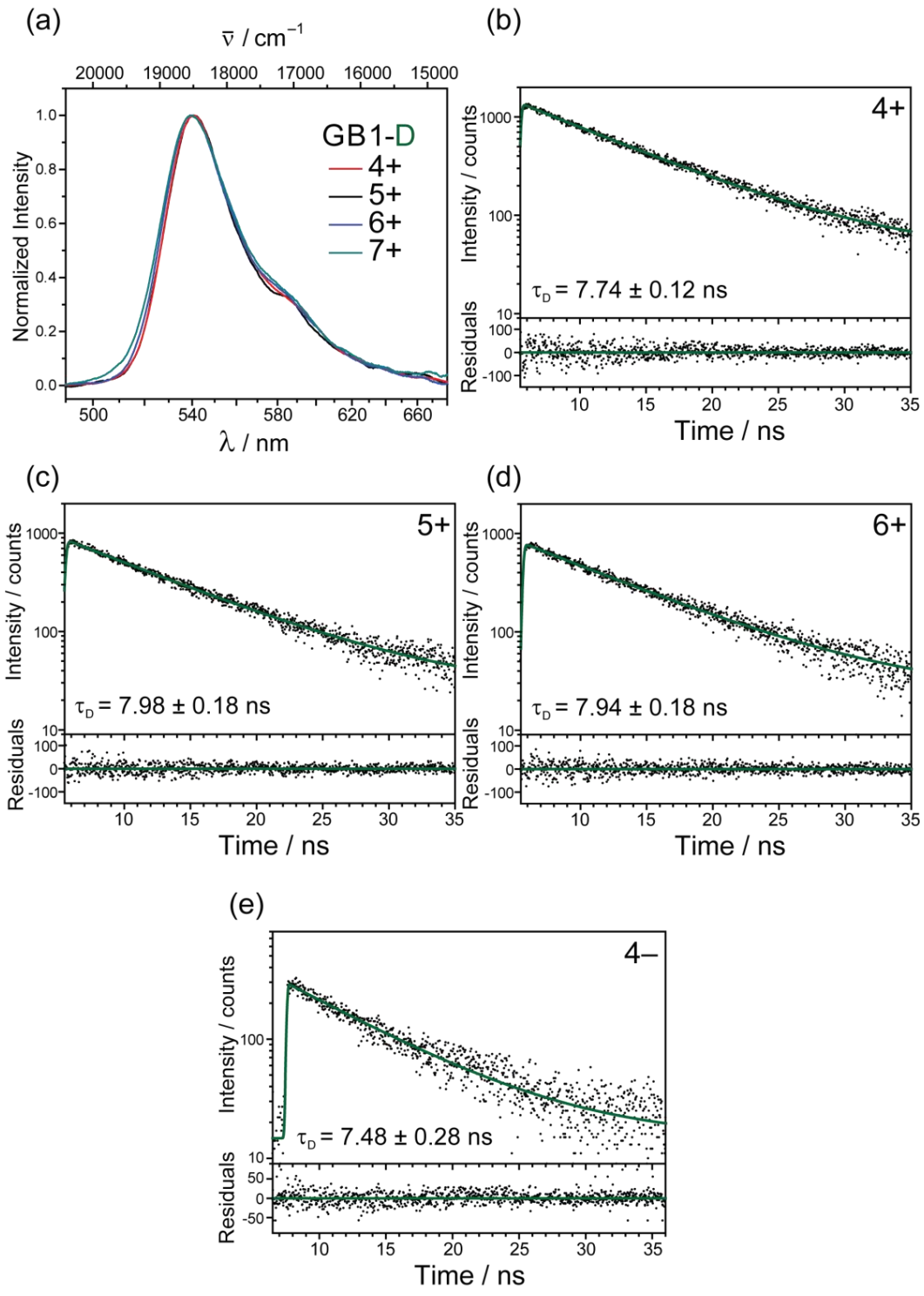

Figure S-3. Charge-state resolved gas-phase fluorescence measurements of the donor-only labeled GB1 construct (GB1-D). Smoothed fluorescence emission spectra (a) for the four cationic charge states measured show similar width and emission maxima (539 ± 2 nm). Fluorescence lifetimes (b–e) were well-fit by single exponential decays. The extracted fluorescence lifetimes from the fit are indicated along with uncertainties (reported as ± three times the standard deviation of the fit).

Determination of FRET Efficiency

From time-resolved fluorescence measurements, the FRET efficiency (E) was calculated according to the usual definition,[5] which relates the efficiency to the fluorescence lifetime of the donor dye in the presence (τ_{DA}) and absence (τ_D) of the acceptor:

$$E = 1 - \frac{\tau_{DA}}{\tau_D}. \quad (1)$$

For a two-component decay, the FRET efficiencies of the two components were computed individually. Note that the potentially broad distributions of distances in partially or fully unfolded GB1 could result in a distribution of fluorescence lifetimes,[5] which we approximate here with one or two discrete components.

From fluorescence emission spectra, the FRET efficiency is most commonly calculated by measurement of the donor intensity in the presence and absence of acceptor, which are each normalized to irradiation power, total exposure time, and concentration. Unfortunately, for the determination of concentration in the present case, we must rely on the ion current generated during the mass spectral scan. Due to mass- and charge-discrimination effects that are known for conversion dynodes,[6] this method is not ideal for quantitation.

Instead, we employ a ratiometric approach,[7] which relates the FRET efficiency to the integrated fluorescence intensities of the donor (I_D) and acceptor (I_A). The FRET efficiency is related to the energy transfer rate (k_t), the radiative decay rate of the donor (k_r), and the sum of all other non-radiative decay rates for the donor (k_{nr}):

$$E = \frac{k_t}{k_t + k_r + k_{nr}} = \frac{1}{1 + \frac{\Phi_A \eta_A I_D}{\Phi_D \eta_D I_A}}, \quad (2)$$

where η_D and η_A are the relative detection efficiencies for the donor and acceptor dyes, and Φ_D and Φ_A are their fluorescence quantum yields. The ratio η_A/η_D was determined to be 1.0. Direct determination of gas-phase quantum yields using our set-up is not possible due to our inability to measure the absorption cross-section. However, it can be estimated using measured gas-phase fluorescence lifetimes and a simplified form of the Strickler-Berg equation,[8] which relates the radiative decay rate of a fluorophore to the index of refraction of the host medium (n) by $k_r \propto n^2$. Using values of $n_{gas} = 1$ and $n_{aq} = 1.33$ (at 530 nm), $k_{r,gas}/k_{r,aq} \approx (1/1.33)^2 = 0.56$. Thus, this simple relation predicts that the gas-phase radiative decay rate is approximately two-fold lower than in aqueous solution. The donor in aqueous solution has a quantum yield of 0.90 and a fluorescence lifetime of 3.8 ns (Atto Tec GmbH). Thus, $k_{r,aq} = \Phi_{aq}/\tau_{aq} = 0.24\ ns^{-1}$, so that $k_{r,gas} \approx 0.56 \times k_{r,aq} =$

0.13 ns^{-1}. Using this estimate for the gas-phase radiative decay rate for the donor dye, and the measured fluorescence lifetime in the absence of acceptor in the gas phase (*i.e.*, 7.9 ± 0.3 ns for GB1-D, Figure S-3b–d), one finds that $\Phi_{gas} = k_{r,gas} \times \tau_{gas} = 1.0$. By the same reasoning, using the measured lifetime of the acceptor in GB1-A (9 ± 1 ns), and its aqueous-phase quantum yield and fluorescence lifetime (0.65 and 3.5 ns, respectively, Atto Tec GmbH), one finds $\Phi_A = 0.9$. This analysis suggests that the two dyes have relatively high fluorescence quantum yields in the gas phase. For the purposes of calculating the FRET efficiency from the measured emission spectra (Table 1), we use the conservative assumption that the gas-phase quantum yields of both dyes lie between their solution-phase values and 1 (*i.e.*, $0.9 < \Phi_D < 1$ and $0.65 < \Phi_A < 1$).

The ratio I_D/I_A, which is central to the calculation of FRET efficiency (Eq. 2), was evaluated for each FRET spectrum according to:

$$\frac{I_D}{I_A} = \frac{\alpha F_D(\lambda_D)}{F_T(\lambda_A) - \beta F_D(\lambda_D)} , \qquad (3)$$

where $F_D(\lambda_D)$ is the fluorescence intensity measured at 539 nm (which is due to donor only), $F_T(\lambda_A)$ is the total fluorescence intensity in the spectrum at 640 nm, α is a correction factor that accounts for differences in spectral width of the donor and acceptor bands, and $\beta F_D(\lambda_D)$ is a correction term for cross-talk in the acceptor channel due to donor emission. The correction factor α was determined to be 1.17, reflecting the fact that the spectral width of the donor is broader than that of the acceptor. The constant $\beta = F_D(\lambda_A)/F_D(\lambda_D)$, was determined to be 0.0633 (*i.e.*, the emission intensity of the donor at 640 nm is about 6% that of the intensity at 539 nm) from the emission spectrum of GB1-D (Figure S-3a).

Estimation of $R_{0,gas}$ for the FRET Dye Pair (ATTO 532 and ATTO 647N)

From the theory developed by Förster, the critical Förster distance R_0 for a pair of oscillating dipoles depends on the spectroscopic properties of the two dyes and on their chemical environment. Namely, $R_0^6 \propto \kappa^2 \Phi_D J n^{-4}$, where κ^2 describes the relative orientation of the donor and acceptor transition dipoles, Φ_D is the donor quantum yield in absence of any acceptor, J is the spectral overlap integral between the donor emission and acceptor absorption profiles, and n is the index of refraction of the medium in which the dyes are embedded. Assessment of each of these parameters in the gas phase is required for accurate determination of $R_{0,gas}$. Unfortunately, some of these quantities cannot be accurately determined in the gas phase.

To estimate the value $R_{0,gas}$ for this dye pair (ATTO 532 and ATTO 647 N), the solution-phase value was used ($R_{0,aq}$ = 59 Å, Atto Tec GmbH) along with correction factors to account for changes to each of the physical quantities on which R_0 depends. Direct determination of the gas-phase donor quantum yield in the absence of acceptor ($\Phi_{D,gas}$) is not possible with our set-up due to our inability to measure its absorption cross-section in the gas phase. However, the measured gas-phase fluorescence lifetime of the donor in GB1-D (~7.9 ns) scales as would be expected from the Strickler-Berg equation,[8] which indicates it has a gas-phase quantum yield near unity (as discussed above). Here, we assume $\Phi_{D,gas}$ to lie between its solution-phase value (0.9, Atto Tec GmbH) and 1; since $R_0 \propto \Phi_D^{1/6}$, this amounts to a relative uncertainty in R_0 of less than 1%. Accurate assessment of J is also not possible using our set-up, since the acceptor absorption maximum lies far above the range of accessible excitation wavelengths (380–530 nm); furthermore, J depends on the absolute magnitude of the acceptor absorption cross-section. The energy difference in the emission maxima of the FRET pair in gaseous GB1-DA (2900 cm^{-1}) is close to that of the bare dyes in aqueous solution (3100 cm^{-1}), which suggests similar spectral spacing in the gas phase as in solution. Further, a spherical cavity model[9] predicts only a slight (~3%) decrease in the magnitude of acceptor absorption cross-section upon transfer to the gas phase. These facts, and considering that $R_0 \propto J^{1/6}$, indicate that changes to the spectral overlap integral likely contribute minimally to changes in R_0. From $R_0 \propto n^{-2/3}$ (using n_{gas} = 1 and n_{aq} = 1.33 at 530 nm), one finds that R_0 is expected to increase by 21% when moving from aqueous solution to the gas phase. Thus, the change in index of refraction is expected to account for the majority of the difference between $R_{0,gas}$ and $R_{0,aq}$, at least insofar as those physical quantities which can be accounted for in a systematic way are concerned. Using these assumptions, and the dynamically averaged value of the orientation factor κ^2 of 2/3 (see below), $R_{0,gas}$ ~ 72 Å for this FRET pair.

We have cautioned that the largest uncertainty in our estimate of $R_{0,gas}$ arises from the uncertainty in the orientation factor κ^2,which describes the relative orientation of the donor and acceptor transition dipoles. The value of κ^2 lies between 0 and 4. Since polarization anisotropy decays, which are used in solution experiments to assess the rotational mobility of the dyes, are not accessible in our gas-phase experiments, we have assumed here the dynamically averaged value of 2/3.[5] While this is a reasonable assumption given the relative flexibility of the dye–protein linkers used here, we cannot rule out the possibility that the dyes are fixed in a relative

orientation that results in κ^2 differing from 2/3; populations of GB1-DA with unusually low κ^2 values would then yield systematically low measured FRET efficiencies, which could be misinterpreted as an indication that GB1 is less compact than it actually is. To assess this possibility, we "back-calculated" values of $R_{0,gas}$ (and hence κ^2), assuming a native-like compactness for the high FRET population present in the 5+ state ensemble of GB1-DA, which shows a FRET efficiency of 0.86. As an upper bound, we use $r_{DA} < 30$ Å for native-like compactness based on the FRET efficiency histograms measured in solution for GB1 (Figure S-4a–c). Using $r_{DA} = 30$ Å, $E = 0.86$, and a Gaussian chain model,[10] one arrives at $R_{0,gas} = 47$ Å (*cf.* our estimate of 72 Å when $\kappa^2 = 2/3$). Assuming this difference is entirely due to an overestimate in κ^2, and using the relation $R_0^6 \propto \kappa^2$, one finds $\kappa^2 = 0.05$. This amounts to a relative orientation of the donor and acceptor transition dipoles that is at most 15° from perpendicular for the majority of these compact GB1 conformers. Although possible, this scenario seems unlikely.

Solution-phase single-molecule FRET experiments

Single molecule FRET experiments were done using a custom-built confocal microscope as described previously[11] equipped with a HydraHarp 400 counting module (Picoquant, Berlin, Germany), and τ-SPAD avalanche photodiodes (PicoQuant). FRET efficiency histograms were recorded at room temperature in appropriate buffer. These were: (1) 25 mM Tris /Tris HCl pH=7.5), (2) 25 mM Glycine/HCl pH=2.5, and (3) an ESI buffer solution containing 0.5 mM sodium phosphate, 30 mM ammonium acetate, and 20% (v/v) methanol. Each solution was supplemented with 144 mM 2-mercaptoethanol and 0.001 % Tween 20.

The donor dye (ATTO 532) was excited with a picosecond pulsed laser operating at 20 MHz (Optical Supercontinuum Systems SCF450-4-20MHz Fianium, Southampton, UK) at 520 nm with an average power of 50 μW. The collected light was filtered using a bandpass filter from Chroma. The concentration of protein was approximately 50 pM. As described previously,[12] photon counts were recorded with a resolution of 16 ps by the counting electronics (time resolution limited by the timing jitter of the detectors used). Identified bursts (total number of counts exceeding 50) were corrected for the background, donor and acceptor quantum yields, and the collection efficiencies in the detection channels.

Figure S-4 shows single-molecule FRET efficiency histograms measured for GB1-DA in pH 7.5 buffer (a), pH 2.5 buffer (b), and the buffer used for nano-ESI for the gas-phase

experiments described (c). In all cases, the histograms show a narrower transfer efficiency distribution peaking at ~0.99, corresponding to inter-dye distances <30 Å. Overall, these data are consistent with the presence of a native GB1 fold under all three solution conditions investigated.

To show that the spectroscopic properties of the dyes are not adversely affected by changes in pH in a way that would confound the GB1 data, FRET efficiency histograms were recorded for a control 20-residue polyproline peptide (pp20). This peptide, containing an N-terminal Gly and a C-terminal Cys residue, was labeled with a maleimide derivative of the donor (ATTO 532) and an NHS ester derivative of the acceptor (ATTO 647N), as described previously.[13] Measured histograms (Figure S-4d–e) show similar efficiency distribution profiles at pH 7.5 (d) and 2.5 (e), which suggests negligible changes to the spectroscopic properties of the dyes.

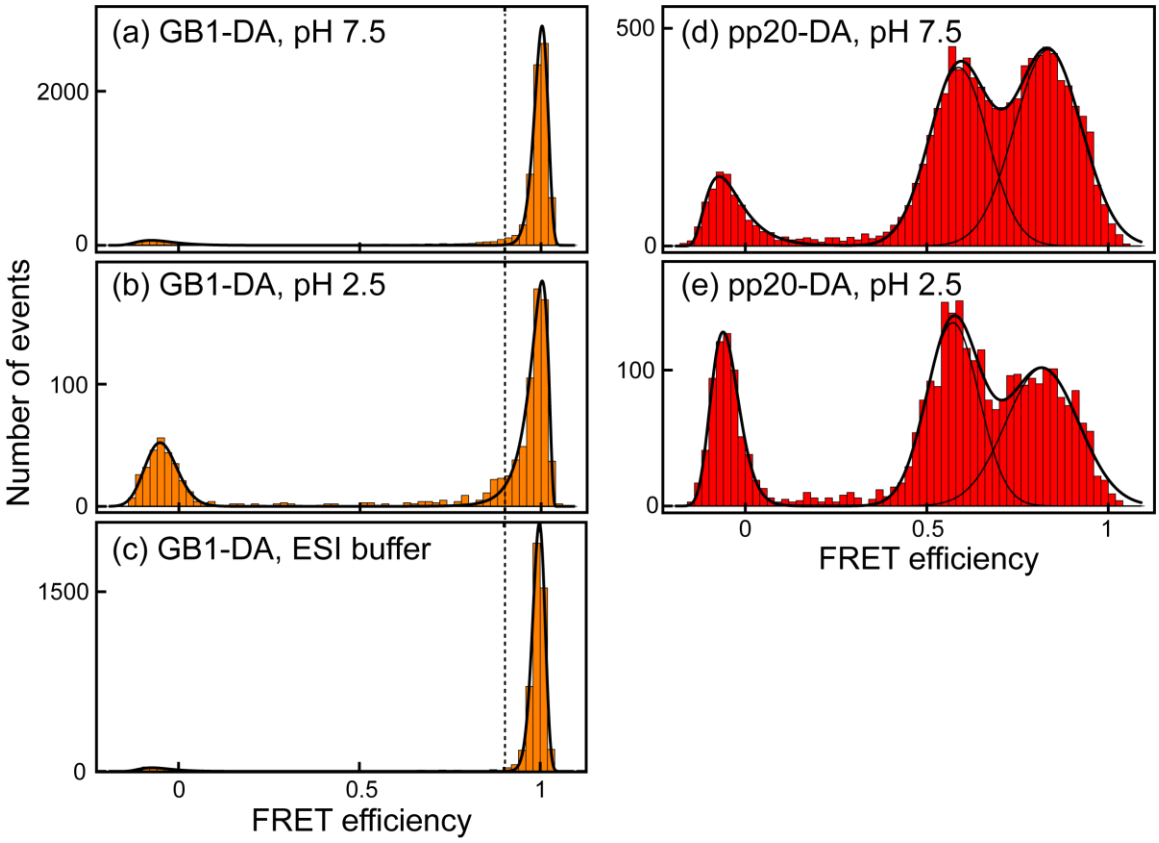

Figure S-4. FRET efficiency histograms for GB1-DA (a–c) and polyproline 20 (d–e) under different solution conditions. 25 mM Tris/Tris HCl was used for measurements at pH=7.5; 25 mM Glycine/HCl was used for measurements at pH=2.5; the ESI buffer contained 0.5 mM sodium phosphate, 30 mM ammonium acetate, and 20% (v/v) methanol. Each solution was supplemented with 144 mM 2-mercaptoethanol and 0.001 % Tween 20. The dashed line at E = 0.9 (a–c) is overlaid for clarity.

References

(1) Selenko, P.; Serber, Z.; Gade, B.; Ruderman, J.; Wagner, G. *Proc. Natl. Acad. Sci. U. S. A.* **2006**, *103* (32), 11904–11909.

(2) Bian, Q.; Forbes, M. W.; Talbot, F. O.; Jockusch, R. A. *Phys. Chem. Chem. Phys.* **2010**, *12* (11), 2590–2598.

(3) Nagy, A. M.; Talbot, F. O.; Czar, M. F.; Jockusch, R. A. *J. Photochem. Photobiol. -Chem.* **2012**, *244*, 47–53.

(4) Czar, M. F.; Jockusch, R. A. *ChemPhysChem* **2013**, *14* (6), 1138–1148.

(5) Lakowicz, J. R. *Principles of fluorescence spectroscopy*; Springer, 2006.

(6) Axelsson, J.; Reimann, C. T.; Sundqvist, B. U. R. *Int. J. Mass Spectrom. Ion Process.* **1994**, *133* (2-3), 141–155.

(7) Deniz, A. A.; Dahan, M.; Grunwell, J. R.; Ha, T. J.; Faulhaber, A. E.; Chemla, D. S.; Weiss, S.; Schultz, P. G. *Proc. Natl. Acad. Sci. U. S. A.* **1999**, *96* (7), 3670–3675.

(8) Strickler, S. J.; Berg, R. A. *J. Chem. Phys.* **1962**, *37*, 814.

(9) Toptygin, D. *J. Fluoresc.* **2003**, *13* (3), 201–219.

(10) Hoffmann, A.; Kane, A.; Nettels, D.; Hertzog, D. E.; Baumgaertel, P.; Lengefeld, J.; Reichardt, G.; Horsley, D. A.; Seckler, R.; Bakajin, O.; Schuler, B. *Proc. Natl. Acad. Sci. U. S. A.* **2007**, *104* (1), 105–110.

(11) Hofmann, H.; Hillger, F.; Pfeil, S. H.; Hoffmann, A.; Streich, D.; Haenni, D.; Nettels, D.; Lipman, E. A.; Schuler, B. *Proc. Natl. Acad. Sci. U. S. A.* **2010**, *107* (26), 11793–11798.

(12) Schuler, B. In *Methods in Molecular Biology*; Bai, Y., Nussinov, R., Eds.; 2007; Vol. 350, pp 115–138.

(13) Schuler, B.; Lipman, E. A.; Eaton, W. A. *Nature* **2002**, *419* (6908), 743–747.